International Journal of Nanomedicine

Dovepress

open access to scientific and medical research

Open Access Full Text Article

ORIGINAL RESEARCH

Nanoparticles Mediated circROBO1 Silencing to Inhibit Hepatocellular Carcinoma Progression by Modulating miR-130a-5p/CCNT2 Axis

Hongyu Meng[1,2,*], Ruixi Li[3,*], Yuankang Xie[1,*], Zhaohong Mo[2], Hang Zhai[2], Guangquan Zhang[3], Guohui Liang[4], Xianjie Shi[3], Boxuan Zhou[1,2]

[1]Department of Hepatobiliary Surgery, The First Affiliated Hospital of Gannan Medical University, Ganzhou, People's Republic of China; [2]Department of Hepatobiliary Surgery, The Third Affiliated Hospital, Sun Yat-sen University, Guangzhou, People's Republic of China; [3]Department of Hepatobiliary and Pancreatic Surgery, The Eighth Affiliated Hospital, Sun Yat-sen University, Shenzhen, People's Republic of China; [4]School of Clinical Medicine, Henan University, Kaifeng, People's Republic of China

*These authors contributed equally to this work

Correspondence: Boxuan Zhou; Xianjie Shi, Email zhoubx3@mail2.sysu.edu.cn; shixianjie301@126.cm

Background: Circular RNAs (circRNAs) are becoming vital biomarkers and therapeutic targets for malignant tumors due to their high stability and specificity in tissues. However, biological functions of circRNAs in hepatocellular carcinoma (HCC) are still not well studied.

Methods: Gene Expression Omnibus (GEO) database and qRT-PCR were used to evaluate expression of circROBO1 (hsa_-circ_0066568) in HCC tissues and cell lines. CCK-8, colony formation, EdU staining, flow cytometry for cell cycle analysis, and xenograft model assays were performed to detect the circROBO1 function in vitro and in vivo. RNA pull-down, RNA immunoprecipitation (RIP), and Luciferase reporter assays were used to investigate the relationship among circROBO1, miR-130a-5p, and CCNT2. More importantly, we developed nanoparticles made from poly lactic-co-glycolic acid (PLGA) and polyethylene glycol (PEG) chains as the delivery system of si-circROBO1 and then applied them to HCC in vitro and in mice.

Results: circROBO1 was obviously upregulated in HCC tissues and cell lines, and elevated circROBO1 was closely correlated with worse prognosis for HCC patients. Functionally, knocking down circROBO1 significantly suppressed HCC cells growth in vitro and in mice. Mechanistically, circROBO1 acted as a competing endogenous RNA to downregulate miR-130a-5p, leading to CCNT2 expression upregulation. Furthermore, miR-130a-5p mimic or CCNT2 knockdown reversed the role of circROBO1 overexpression on HCC cells, which demonstrated that circROBO1 promoted HCC development via miR-130a-5p/CCNT2 axis. In addition, we developed nanoparticles loaded with si-circROBO1, named as PLGA-PEG (si-circROBO1) NPs, which significantly prevented the proliferation of HCC cells, and did not exhibit apparent toxicity to major organs in vivo.

Conclusion: Our findings firstly demonstrate that circROBO1 overexpression promotes HCC progression by regulating miR-130a-5p/CCNT2 axis, which may serve as an effective nanotherapeutic target for HCC treatment.

Keywords: nanoparticles, hepatocellular carcinoma, circROBO1, cell proliferation, drug delivery

Introduction

The HCC, a major pathohistological subtype of primary liver cancer, is one of main cause for cancer-associated death in many countries.[1] Generally, HCC patients are asymptomatic at the early stage, when patients diagnosed with HCC at the advanced stage are usually ineligible for therapeutic surgery.[2] Additionally, although survival time in some HCC patients who meet the surgical requirement could be improved, their 5-year overall survival rates remain to be unsatisfactory (about 50%).[3] Hence, it is urgent to identify novel biomarkers to enhance the early diagnosis rate and overall survival (OS) of HCC patients.

CircRNAs have been identified involved in the development of various types of cancers, comprising lung cancer, breast cancer, and HCC.[4] CircRNAs form a special covalently closed-loop structure, thus endowing circRNAs more

Received: 9 December 2022
Accepted: 7 March 2023
Published: 30 March 2023

stable character than their linear transcripts from the host gene. Recently, mounting evidence has revealed that this kind of RNAs might adjust gene expression at three different levels: transcriptional, post-transcriptional, and translational level, respectively.[5,6] Circular exonic RNAs which mainly accumulate in cytoplasm may play the role of miRNA sponges to lower their expression, ultimately leading to enhanced expression of these miRNA target genes.[5,7,8] However, circular intronic RNAs or exon-intron RNAs usually appear in the nucleus and can adjust the transcription process.[9] These findings indicate that circRNAs may be involved in different pathological processes.

Accumulating studies have demonstrated that circRNAs were deregulated in HCC tissues and regulated the malignant behavior of tumor cells by targeting different miRNAs, thereby exerting impact on the HCC progression.[4] For instance, circSEC62 promoted SNRPA levels by silencing miR-625-5p and affected HCC microvascular invasion.[10] Since ROBO1 was aberrant expressed in various cancers,[11–13] but the function of ROBO1 derived circRNAs in cancers still remained unclear. Among 40 circRNAs derived from parental gene ROBO1, only hsa_circ_0124696 (back splicing exon 5–8 of ROBO1) was identified to regulate the liver metastasis of breast cancer.[14] However, less is known about ROBO1 derived from circRNAs in HCC. Additionally, the enrichment of circRNAs in the cytoplasm could function by sponging miRNAs to exert a significant role in cancer development.[15,16] Previous study indicated that miR-130a-5p mimic inhibited the progression of non-small cell lung cancer by suppressing cell proliferation and inducing cell apoptosis.[17] CCNT2, an element of the P-TEFb complex, is indispensable for initiation and extension of transcription mediated by RNA polymerase II.[18] A recent study reported that overexpression of CCNT2 reversed the arrest of G0/G1 cell cycle in AML cells.[19] Hence, we wonder whether miR-130a-5p/CCNT2 axis plays a role in HCC progression.

Small interfering RNAs (siRNAs) are very important in nucleic acid treatment process due to their special RNAi-triggering activity.[20] For the great significance of effective delivery in transporting siRNA to target cells and tissues, various materials have been developed to deliver siRNAs, such as lipids, exosomes, polymeric micelles, and polymeric nanoparticles (NPs). For example, Ye et al reported that exosomes with decreased hsa_circ_0000069 could inhibit malignant transformation of pancreatic cancer.[21] Additionally, NPs can also be loaded with active compounds entrapped onto the polymeric core. NPs formulated with poly lactic-co-glycolic acid (PLGA) copolymer are promising options for cancer therapy, which are made from biocompatible and biodegradable constituents with non-toxicity.[22,23] Furthermore, NPs display a highly selective targeting and uptake adequacy in cancer cells rather than healthy ones or the mononuclear phagocytic system, which can be achieved through cell-specific ligands and attachment of polyethylene glycol (PEG) chains on the nanoparticles surface.[24] Importantly, NPs for drug delivery application show great prospects in HCC therapeutic treatment. For instance, Rahman et al illustrated that systemically optimized resveratrol-loaded cationic solid lipid nanoparticles (RV-c-SLNs) exhibited enhanced anti-HCC action as well as high accumulation to tumor.[25]

In this study, we illustrate a novel mechanism that circROBO1 promotes tumor cells growth by modulating miR-130a-5p/CCNT2 axis to promote HCC progression. Moreover, PLGA-based si-circROBO1 nanoparticles significantly suppress the proliferation of HCC cells, which provide a potential nanotherapeutic approach for future HCC therapy.

Materials and Methods

Patients and Samples

We collected 118 tissue samples diagnosed with HCC between 2013 and 2017 in the First Affiliated Hospital of Gannan Medical University. All patients signed written informed consent. The recruited HCC patients who had received chemotherapy or other treatments before curative surgery were excluded. All surgically excised specimens were rapidly frozen in liquid nitrogen. The study was conducted in accordance with the Declaration of Helsinki and approved by the First Affiliated Hospital of Gannan Medical University (LLSC-2022121301).

Cell Culture

We purchased HCC cell lines (HepG2, SMMC-7721, and Huh-7) and the normal hepatic cell line LO2 from Chinese Academy of Sciences (Shanghai, China). HCCLM9 was obtained from Liver Cancer Institute (Fudan University, China). DMEM including 10% FBS, 100 μg/mL streptomycin, and 100 U/mL penicillin was utilized to culture these cells at 37°C with 5% CO_2.

Microarray-Based circRNA Expression Profile

CircRNAs expression data of HCC (GSE156088, including 59 paired HCC tissues and para-cancerous normal tissues) were obtained from the GEO database (https://www.ncbi.nlm.nih.gov/geo/). Subsequently, we further preprocessed expression profiling data of circRNAs based on the R Limma package. Finally, differentially expressed circRNAs were chosen based on following judgement standard: $|\log_2 FC|>1$ and p-value <0.05.

qRT-PCR

TRIzol Reagent and NanoDrop2000 were, respectively, applied to isolate and quantify total RNA, and then the obtained RNA was reverse-transcribed into cDNA using a reverse transcription kit (TakaRa, Japan) or miRNA first-strand cDNA synthesis kit (GeneCopoeia, China). Quantitative RT-PCR detection (qRT-PCR) was conducted based on SYBR Green PCR Master Mix (TakaRa, Japan). Relative expression of RNAs was determined by $2^{-\Delta\Delta Ct}$ method. The primers for PCR were displayed in Supplementary Table S1.

Plasmid Construction, Stable Cell Line Generation, and Oligonucleotide Transfection

For construction of sh-circROBO1, si-circROBO1 sequence was cloned into the pLKO.1 vector. For circROBO1 overexpression, the cDNA of circROBO1 was cloned into pLO-ciR vector. For generation of stable cell lines, lentiviruses containing the above vectors were generated in HEK 293T cells as previously described.[26] miR-130a-5p mimic, miR-130a-5p inhibitors, and negative controls were synthesized by Generay Biotech (Shanghai, China). The oligonucleotide transfection was performed by LipofectamineTM RNAiMAX Reagent (Invitrogen, USA) according to the corresponding recommendation. All oligonucleotide sequences used were displayed in Supplementary Tables S2–S5.

CCK-8 Assay

Cell proliferation detection was performed CCK-8 kit (Beyotime, Shanghai). Briefly, cells at logarithmic growth period were harvested and then seeded into 96-well plates. After culturing for 0, 24, 48, and 72 h, 10 μL CCK8 reaction solutions were added and the optical density (OD) index at 450 nm was captured on a microplate reader (Biorad, USA).

Colony Formation Assay and EdU Assay

HCC cells were diluted and seeded (10^3 cells per well in 6 well plates). After 2 weeks, cells were fixed and then stained with 0.4% crystal violet (Beyotime, China). Subsequently, cells were thoroughly washed with PBS. The colony number in each well was counted under light microscopy.

We also conducted 5-Ethynyl-2-deoxyuridine (EdU) incorporation assay to detect HCC cells proliferation. In brief, we seeded HCC cells and then added 10 μM EdU (Beyotime, China) into plates for 2 h at 37°C. Subsequently, we fixed cells for 15 min at room temperature (RT). Then, 0.5% Triton X-100 was used to permeabilize cells and then incubated with a 1×Apollo reaction cocktail for half an hour. Finally, the cell nuclei was stained for 15 min, and the images were captured by fluorescence microscopy.

RNase R Digestion Assay and Actinomycin D Assay

For RNase R digestion assay, we first equally divided the RNA sample of HCC cells: one was applied for RNase R digestion, the other one was used as control. Samples in RNase R treated group were incubated at 37°C for 15 min. The levels of circROBO1 and ROBO1 mRNA were detected through qRT-PCR.

For actinomycin D assay, we seeded HCC cells into 6-well plates (2×10^5 cells/well). Then, cells were treated with actinomycin D (1 μg/mL) and harvested after 0, 4, 8, 16, and 24 h. The levels of circROBO1 and ROBO1 mRNA were analyzed by qRT-PCR and normalized to the value of the 0-h group.

Subcellular fraction Assay

For subcellular fraction assay, we extracted the nuclear and cytoplasmic fractions from HCC cells based on PARIS Kit (Invitrogen, USA) according to the manufacturer's recommendation. The levels of circROBO1, ROBO1 mRNA, β-actin, and U6 were determined by qRT-PCR.

Dual-Luciferase Reporter Assay

We predicted binding sites between miR-130a-5p and circROBO1 or CCNT2 3'-UTR based on the starbase v3.0 (http://starbase.sysu.edu.cn/) database. We inserted the wild-type (WT) and mutant (MUT) sequences of circROBO1 or CCNT2 3'-UTR containing miR-130a-5p binding sites into the downstream reporter vector. For luciferase assay, HCC cells were co-transfected with miR-130a-5p mimic, miR-130a-5p inhibitor, miR-NC, and reporter vector, respectively. After incubating for 48 h, luciferase activity was detected.

RNA Pull-Down Assay

The biotin-labeled miR-130a-5p probe (Bio-miR-130a-5p) and control probe (Bio-control) were constructed by Generay (Shanghai, China). These probes were transfected into cells for 48 h. Then, we incubated these cell lysates with streptavidin magnetic beads. Finally, the immune-precipitated RNA was extracted by the proteinase K-chloroform method. The probe sequences for RNA pull-down assay were displayed in Supplementary Table S6.

RNA Immunoprecipitation (RIP) Assay

We applied a Magna RNA immune-precipitation kit (Millipore) to verify the interaction between miR-130a-5p and circROBO1 in HCC cells. In brief, HCC cells at 80% confluence were incubated with RIP solution. Then, cell lysates were incubated with anti-AGO2 (Cat#ab186733, Abcam) or IgG (Cat#ab172730, Abcam) antibody for 16 h at 4°C. The immune-precipitated RNA was extracted by the proteinase K-chloroform method.

Xenograft Tumor Model

All animal experiments were approved by the Ethics Committee of Gannan Medical University (2020018) and conducted in accordance with Guidelines for the Care and Use of Laboratory Animals of the National Institutes of Health. Four-week-old male nude mice were randomized to each experimental group. 10^6 HCC cells transduced with lentivirus carry control or circROBO1 shRNA and with or without circROBO1 overexpression were dispersed in 100 μL PBS. Then, HCC cells suspension was injected subcutaneously into the back of nude mice. To measure tumor volume, the long and short diameters (represented by L, W) of xenograft tumors were measured every 4 days using a vernier caliper. The tumor volume was determined based on formula of $L \times W^2/2$. After 28 d, the experiment animals were euthanized and collected tumor samples.

Preparation of PLGA-PEG (si-circROBO1) Nanoparticles (NPs)

We used double emulsion solvent diffusion strategy to prepare NPs as previously described.[27] First, we mixed spermidine (Sigma-Aldrich) with reconstituted si-circROBO1 (dissolved in DEPC water) (polyamine amine groups: siRNA phosphate groups=8:1). The obtained mixtures were reacted at RT for 15 min to form si-circROBO1/spermidine mixture. Meanwhile, we dissolved 10 mg poly (L-lactide-co-glycolide)-b-poly (ethylene glycol)-carboxylic acid (PLGA-PEG-COOH) in 500 μL of dichloromethane. Subsequently, we added dichloromethane solution to si-circROBO1/spermidine complex with a probe sonicator. Next, we collected primary emulsion and added dropwise to 4 mL of an aqueous phase and then emulsified for 60 second. Then, the second emulsion was continuously stirred for 4 h at RT to evaporate the organic solvent. Finally, we collected NPs by centrifugation and washed twice with DEPC water.

Pharmacokinetic Assay and Biodistribution of PLGA-PEG (si-circROBO1) NPs in Mice

Pharmacokinetic (PK) assay was used as previously described,[28,29] 4-week-old male nude mice were divided into two groups (three mice in each group) and injected free Cy-5 si-circROBO1 or PLGA-PEG (Cy-5 si-circROBO1) NPs at 1nmol siRNA dose per mouse via tail vein. At different point in times (0, 5,10,15, 30, 60, 120, 240, 480, 960 min), blood samples were obtained. After measured at different time intervals with a microplate reader, Cy-5 fluorescence intensity in blood was used to describe PK.

Biodistribution experiment in the HCC tumor model was performed as previously described,[30] HCCLM9 cells derived nude mice received free Cy-5 si-circROBO1 or PLGA-PEG (Cy-5 si-circROBO1) NPs. After 24 h of injection,

organs and tumors were obtained and observed with the IVIS Lumina III In Vivo Imaging System. Image J software was used to analyze the Cy-5 fluorescence intensity.

Evaluation of PLGA-PEG (si-circROBO1) NPs for Antitumor Efficacy and Toxicity in Mice

To investigate the antitumor efficacy of PLGA-PEG loaded with si-circROBO1 NPs in vivo, nude mice HCC models were constructed. Under condition of the tumors grow to about 50 mm^3 (day 7), we injected PLGA-PEG (si-circROBO1) NPs or PLGA-PEG (siRNA control) NPs at a dose of 700 μg/kg through the tail vein every 3 days for 7 cycles. At day 31, mice were sacrificed. The major organs were harvested and fixed with for hematoxylin–eosin (H&E) staining examination. Blood biochemical indicators, including ALT, AST, BUN, and Cr were also analyzed using corresponding kits.

Statistical Analysis

We used GraphPad Prism 9.0 to perform the statistical analysis. Data were displayed as mean ± standard deviation with three repeated experiments. The *t*-test or ANOVA test was applied to determine the differences. The relationship between miR-130a-5p and CCNT2 in HCC tissues was assessed via Pearson's correlation coefficients. $P < 0.05$ was regarded as existing significant.

Results

CircROBO1 Was Significantly Upregulated in HCC

For the identification of differential expression of circRNAs between HCC and paired adjacent tissues, we analyzed GEO dataset (GSE156088) with $|\log_2 \text{fold change}|>1$ and $P < 0.05$ as screening conditions. In total, we identified 24 upregulated circRNAs and 15 downregulated circRNAs in HCC tissues compared to paracancerous tissues (Figure 1A). Finally, we chose circROBO1 (hsa_circ_0066568) for further study due to high expression in HCC tissues and high conservation between human and mouse (Supplementary Figure 1A). Subsequently, upregulated circROBO1 was also validated in a cohort of 20 cases HCC patients using qRT-PCR (Figure 1B). In addition, we further examined the expression of circROBO1 in human normal hepatocyte cell line (LO2) and HCC cells, and found that HCC cells exhibited higher circROBO1 levels than LO2 cells (Figure 1C).

CircROBO1 derived from exon 4, exon 5, and exon 6 of the ROBO1 gene with 388nt in length (Figure 1D). As expected, we found that circROBO1 was stabler than the corresponding linear mRNA by Ribonuclease (RNase) R and actinomycin D assays (Figure 1E and F). Furthermore, subcellular fractionation assays indicated that circROBO1 mainly existed in cytoplasm (Figure 1G).

To further investigate the prognostic value of circROBO1, 118 HCC patients were divided into circROBO1-low and -high -expression group based on the median value of circROBO1 in qRT-PCR, and K-M survival analysis suggested that HCC cases with higher circROBO1 had worse OS and RFS than those with lower expression of circROBO1 (Figure 1H). Overall, these results suggest that circROBO1 is obviously upregulated in HCC and may serve as an unfavorable prognostic factor.

CircROBO1 Overexpression Promoted HCC Growth

To investigate the oncogenic role of circROBO1 in HCC, stable knocking down circROBO1 HCCLM9 cells were constructed using short hairpin RNAs, which targeted the back-spliced junction site of circROBO1. Meanwhile, stable overexpressing circROBO1 SMMC-7721 cells were constructed by lentiviral transduction (Figure 2A). Subsequently, CCK-8, colony formation and EdU staining assays consistently demonstrated that the proliferation of HCCLM9 cells was significantly suppressed when circROBO1 was silenced, while the opposite results were observed when circROBO1 was overexpressed in SMMC-7721 cells (Figure 2B–D, Supplementary Figure 2A and B). Moreover, flow cytometry for cell cycle analysis suggested that the number of G2/M phase cells decreased after knocking down circROBO1, while overexpression of circROBO1 elevated the numbers of G2/M phase cells (Supplementary Figure 2C and D). Furthermore, we also successfully established a xenograft tumor model of HCC via the incubation of HCC cells into nude mice for the confirmation of carcinogenic effect of circROBO1 in vivo. The results showed that tumor growth was

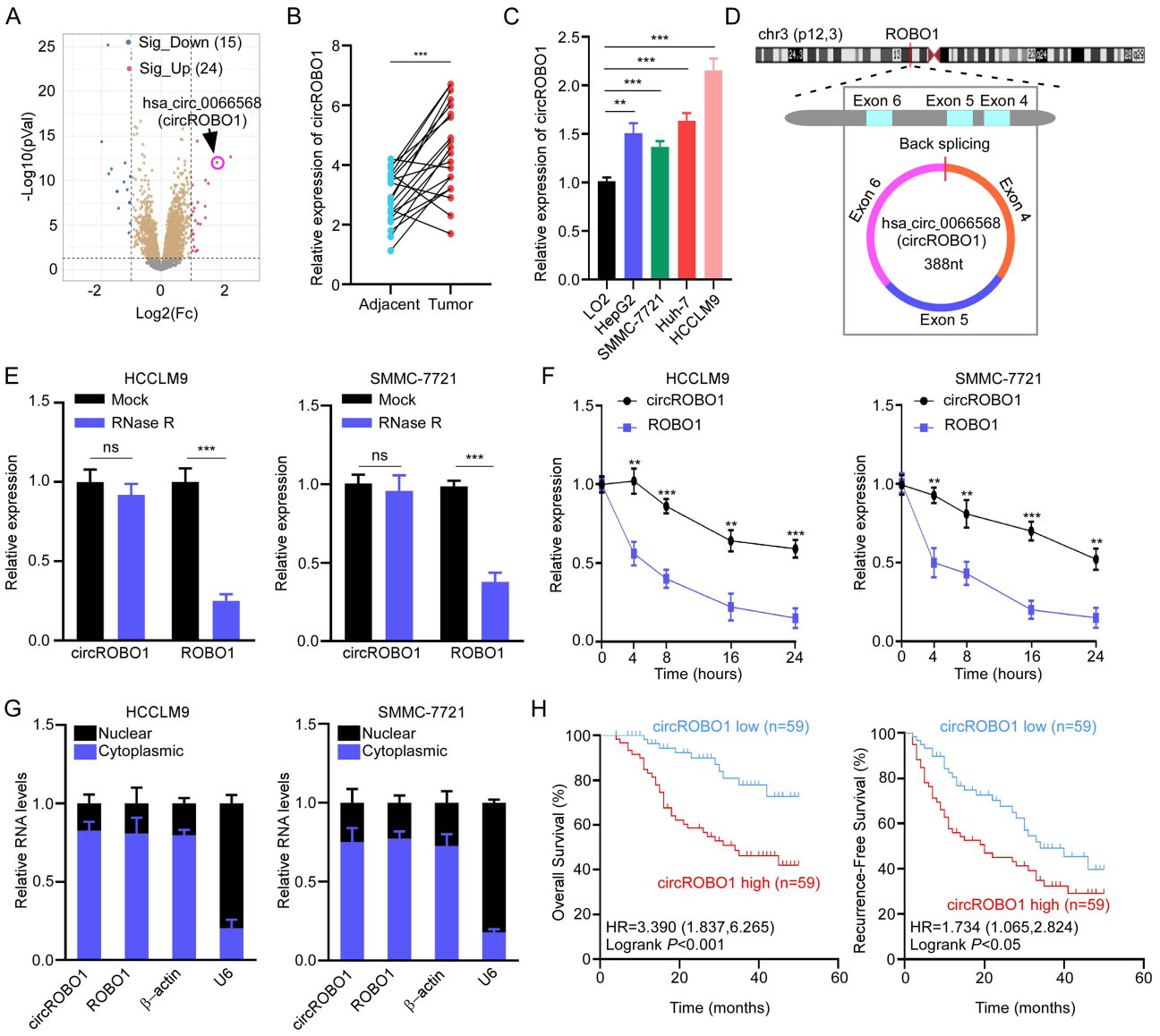

Figure 1 CircROBO1 is overexpressed in HCC. (**A**) Volcano plot showing differentially expressed circRNAs between tumor tissues and paired adjacent tissues from GSE156088 dataset. (**B**) Analysis of circROBO1 expression in 20 paired HCC tissues and adjacent tissues by qRT-PCR. (**C**) qRT-PCR analysis of circROBO1 expression in HCC cell lines and normal hepatic cell line LO2. (**D**) Schematic illustration showing the genomic loci of the ROBO1 gene and the circROBO1 is back-spliced from exon 4 to exon 6 of ROBO1. (**E**) qRT-PCR analysis for the resistance of circROBO1 and linear ROBO1 to RNase R in HCCLM9 and SMMC-7721 cells. The mock treatment is the negative control. (**F**) Actinomycin D assay to evaluate the stability of circROBO1 and ROBO1 mRNA in HCCLM9 and SMMC-7721 cells. (**G**) Nuclear-cytoplasmic fractionation assay was performed to examine the subcellular distribution of circROBO1 in HCCLM9 and SMMC-7721 cells. β-actin and U6 were used as cytoplasmic and nuclear positive controls, respectively. (**H**) Kaplan-Meier's survival curves showing the correlations between circROBO1 expression and OS or RFS. Log rank test was used. Data were presented as means ±SD. ***P*<0.01; ****P*<0.001.

notably inhibited in circROBO1 silenced groups, while promoted in circROBO1 overexpression group (Figure 2E). Collectively, the results indicate that circROBO1 overexpression promotes the proliferative performance of HCC cells in vitro and in animals.

CircROBO1 Promoted HCC Cells Proliferation by Sponging miR-130a-5p

Since circRNAs usually functioned as miRNA sponges by competitively binding to specific miRNAs,[4,31] we searched databases including Circbank and Starbase to explore possible target miRNAs of circROBO1 and found miR-130a-5p was the only intersection between the two databases that potentially bound to circROBO1 (Figure 3A). Subsequently, RNA pull-down assays with biotinylated miR-130a-5p and control probe were

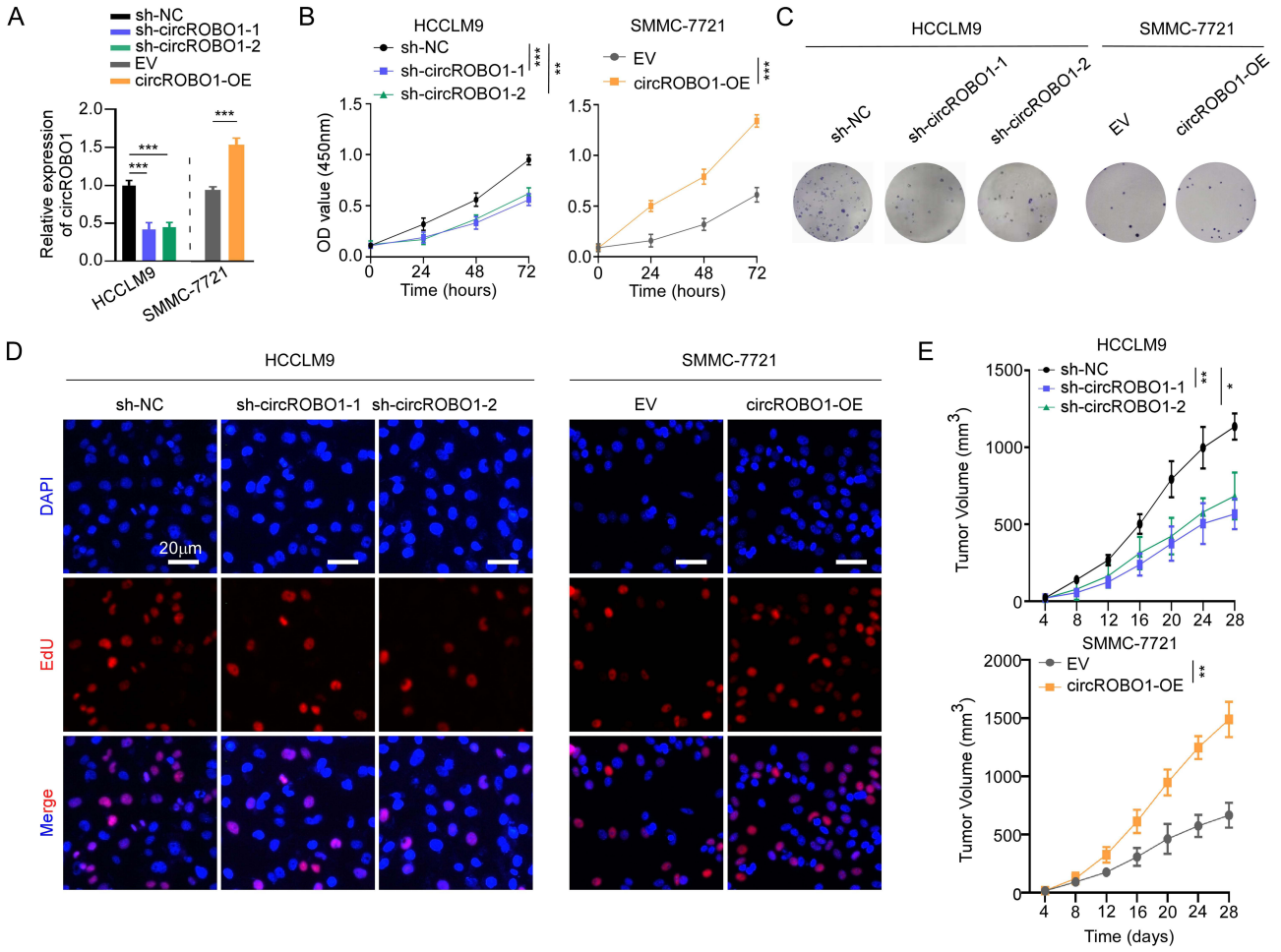

Figure 2 CircROBO1 overexpression promotes the proliferation of HCC cells. (**A**) The relative expression of circROBO1 in HCCLM9 and SMMC-7721 cells as indicated treatments was analyzed by qRT-PCR. (**B**–**D**) Cell proliferative ability was evaluated by CCK-8 (**B**), colony formation (**C**) and EdU (**D**) assays in HCCLM9 and SMMC-7721 cells as indicated treatments. Scale bar, 20 μm. (**E**) A xenograft tumor model was established via subcutaneously injecting circROBO1 silenced or overexpressed HCC cells. Tumor volume was measured at different time-points. Data were presented as means±SD. **P*<0.05; ***P*<0.01; ****P*<0.001.

conducted, and the results indicated that circROBO1 was significantly enriched (Figure 3B). Furthermore, we constructed full-length circROBO1 sequence (circROBO1-WT) and circROBO1 sequences with mutant binding sites (circROBO1-MUT) followed by luciferase reporter assay (Figure 3C). Our results demonstrated that miR-130a-5p mimic and inhibitor significantly reduced and increased luciferase activity of circROBO1-WT plasmid, but not that of circROBO1-MUT plasmid, respectively (Figure 3D). In addition, RNA immunoprecipitation (RIP) assays using argonaute2 (AGO2) antibody showed that circROBO1 and miR-130a-5p could both be enriched (Figure 3E). These results suggest that circROBO1 may be seen as a binding platform for miR-130a-5p and AGO2.

Next, TCGA database was used to evaluate expression levels of miR-130a-5p, and data demonstrated that miR-130a-5p expression was markedly downregulated in HCC samples (Figure 3F). To deeper research whether the influence of circROBO1 on HCC cells proliferation could be reversed by miR-130a-5p, we conducted a series of rescue assays. Colony formation and EdU assays consistently showed that the suppressed proliferation induced by knockdown of circROBO1 in HCCLM9 cells could be blocked by miR-130a-5p inhibitor, and the increased proliferation induced by circROBO1 overexpression of SMMC-7721 cells could be retarded by miR-130a-5p mimic (Figure 3G and H). Collectively, our results suggest that circROBO1 may function as a sponge for miR-130a-5p.

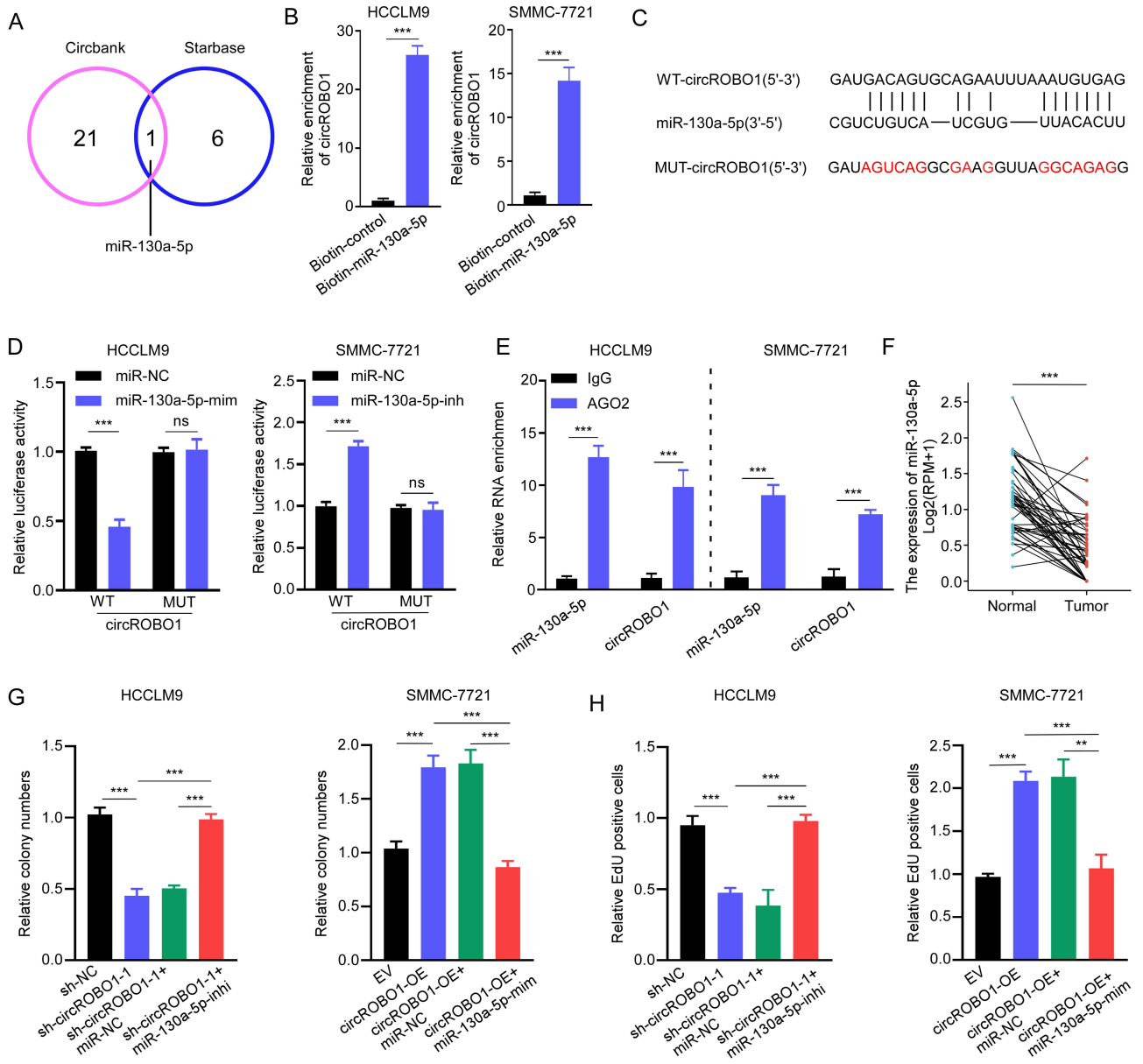

Figure 3 CircROBO1 functions as a sponge for miR-130a-5p. (**A**) Venn diagram showing potential target miRNAs of circROBO1 as predicted by Circbank and Starbase databases. (**B**) RNA pull-down with a biotin-labeled miR-130a-5p probe was conducted in HCC cell lines, the enrichment of circROBO1 was detected by qRT-PCR. (**C**) Schematic illustration of full length of wide type (WT) circROBO1 or a version where the miR-130a-5p-binding sites was mutated (MUT). (**D**) The luciferase activity of WT circROBO1 or MUT circROBO1 after transfection with miR-130a-5p mimic or inhibitor in HCCLM9 and SMMC-7721 cells, respectively. (**E**) RIP assay was performed to detect circROBO1 and miR-130a-5p binding to AGO2. (**F**) The expression of miR-130a-5p in HCC tissues and paired adjacent tissues from TCGA database. (**G** and **H**) The cell proliferative ability was detected in HCC cells as indicated treatments by colony formation (**G**) and EdU (**H**) assays. Data were presented as means ±SD. ***P*<0.01; ****P*<0.001.

miR-130a-5p Inhibited HCC Proliferation by Negatively Regulating CCNT2 Expression

Given that miRNAs regulated target genes expression by interacting with the 3′-UTR,[32] hence we further investigated the potential target genes of miR-130a-5p in HCC. Data from MicroT (top 400 according to miTG score), miRDB (top 400 according to Target Score) and Starbase (top 400 according to AgoExpNum rank) were downloaded and further used to analyze, the results showed that ANKHD1, TNRC6B, PTP4A2, CCNT2, CFL2, SIX4, and CPEB2 were the potential target genes of miR-130a-5p (Figure 4A). Among them, PTP4A2, CCNT2, and CFL2 were selected through top 3 "AgoExpNum" rank of Starbase database. Additionally, TCGA database showed that CFL2 was downregulated, but CCNT2 and PTP4A2 were upregulated in HCC tissues (Figure 4B). CCNT2 was reported to regulate cell proliferation in

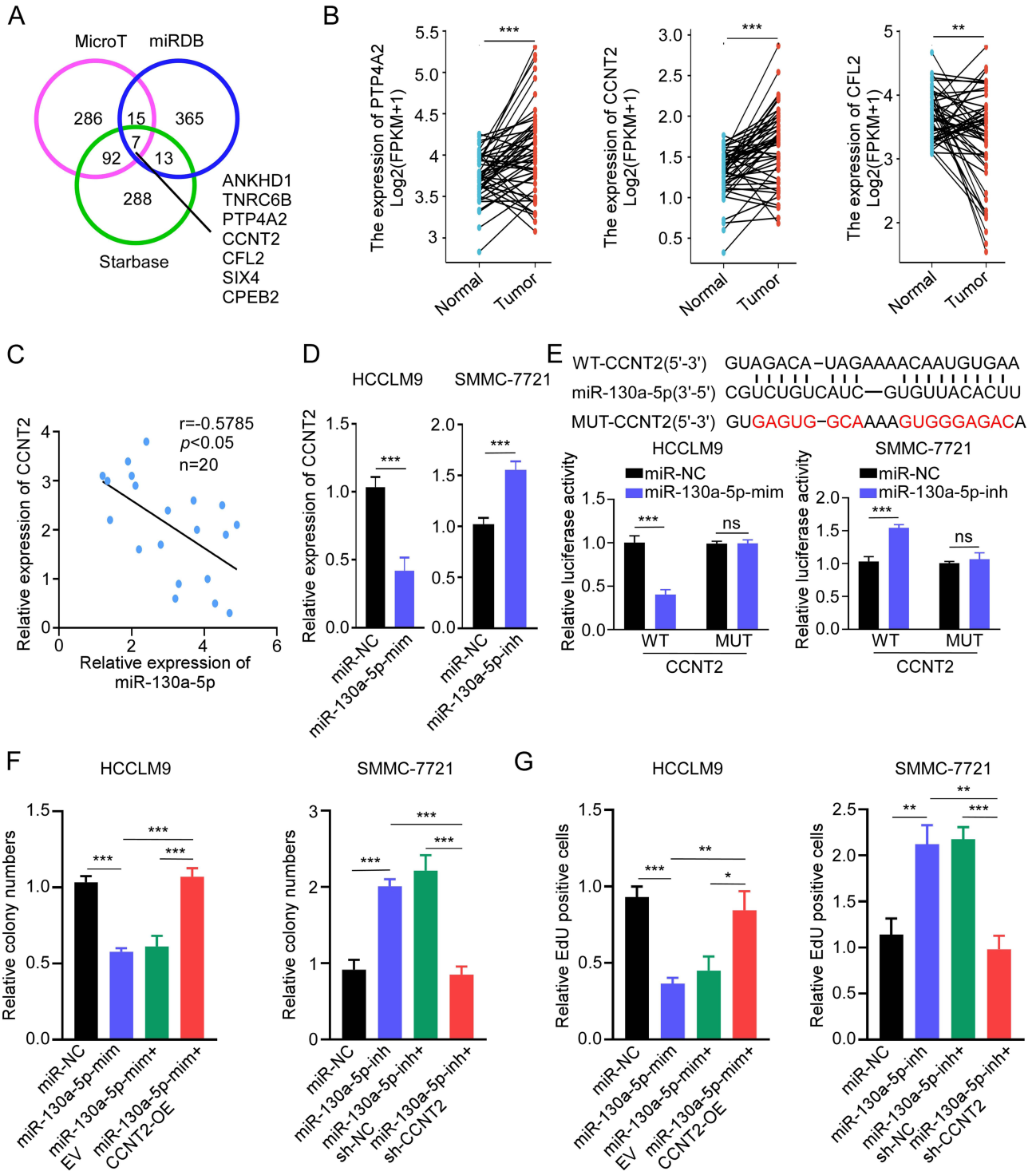

Figure 4 MiR-130a-5p inhibits HCC proliferation by negatively regulating CCNT2 expression. (**A**) Venn diagram showing the overlapping target genes of miR-130a-5p predicted by MicroT, miRDB and Starbase databases. (**B**) The expression of PTP4A2, CCNT2, and CFL2 in HCC tissues and paired adjacent tissues from TCGA database. (**C**) Pearson's correlation analysis of CCNT2 and miR-130a-5p expression in 20 cases HCC tissues. (**D**) The relative expression of CCNT2 was detected in HCCLM9 and SMMC-7721 cells after transfection of miR-130a-5p mimic or miR-130a-5p inhibitor by qRT-PCR. (**E**) Schematic illustration of full length of CCNT2 3'-UTR wide type (WT) or a version where the miR-130a-5p binding sites were mutated (MUT). The luciferase activity of CCNT2 3'-UTR WT or CCNT2 3'-UTR MUT after transfection of miR-130a-5p mimics or inhibitor in HCCLM9 and SMMC-7721 cells, respectively. (**F** and **G**) The cell proliferative ability of HCCLM9 and SMMC-7721 cells as indicated treatments was detected by colony formation (**F**) and EdU (**G**) assays. Data were presented as means ±SD. **P*<0.05; ***P*<0.01; ****P*<0.001.

https://doi.org/10.2147/IJN.S399318 DovePress

multiple cancers,[19,33] therefore we finally selected CCNT2 as a potential target gene of miR-130a-5p for further study. Surprisingly, Pearson's analysis result implied that there was a negative correlation between miR-130a-5p and CCNT2 expression in HCC tissues (Figure 4C). Furthermore, we found that CCNT2 expression was promoted and repressed by miR-130a-5p inhibitor and mimic in HCC cells, respectively (Figure 4D). To further verify that miR-130a-5p interacted with CCNT2, a luciferase reporter plasmid carrying CCNT2 sequences (wild-type (WT) or mutant (MUT)) was constructed. Luciferase reporter assays showed that miR-130a-5p mimic and inhibitor reduced and increased the luciferase activity, respectively, from tumor cells transfected with CCNT2-WT but not in CCNT2-MUT group (Figure 4E).

Previous studies have reported that miR-130a-5p functioned as a tumor suppressor in HCC,[34] and our study consistently confirmed miR-130a-5p inhibitor and mimic promoted and suppressed the proliferation of HCC cells, respectively. More importantly, the promoted proliferation induced by miR-130a-5p inhibitor and inhibited proliferation induced by miR-130a-5p mimic in HCC cells were blocked by CCNT2 knockdown and overexpression, respectively (Figure 4F and G). Together, the results suggest that miR-130a-5p could curb proliferation of HCC cells via directly inhibiting the expression of CCNT2.

CircROBO1 Promoted HCC Proliferation by Upregulating CCNT2 Expression

To further investigate whether circROBO1 promoted the proliferation of HCC cells by upregulating CCNT2, we constructed a co-transfection system of circROBO1 shRNA and CCNT2 overexpression plasmid in HCCLM9 cells as well as circROBO1 overexpression and sh-CCNT2 plasmid in SMMC-7721 cells, respectively. qRT-PCR results showed that CCNT2 knockdown could decrease the increased CCNT2 expression in upregulated circROBO1 SMMC-7721 cells, while overexpression of CCNT2 could rescue the decreased CCNT2 level in silenced circROBO1 HCCLM9 cells (Figure 5A). Subsequently, CCK-8, colony formation, and EdU assays implied that transfection of sh-circROBO1 weakened cells proliferation, which these effects could be blocked by CCNT2 overexpression (Figure 5B–D). However, knocking down CCNT2 significantly reversed the promoting cell proliferation in overexpressed circROBO1 cells (Figure 5B–D). Taken together, our data indicate that circROBO1 promotes HCC cells proliferation by upregulating CCNT2 expression.

The Biological Feature of PLGA-PEG (si-circROBO1) NPs

To investigate the possibility of circROBO1 as a treatment target for HCC, a PLGA-based nanoplatform encapsulating si-circROBO1 was constructed. The PEGylated PLGA NPs loaded with si-circROBO1 and G0-C14, named as PLGA-PEG (si-circROBO1) NPs, were prepared by employing the method of double emulsion solvent diffusion (Figure 6A). The stability of NPs could be improved by PEGylated PLGA via reducing their interactions with serum proteins.[35] G0-C14 compound can be combined with siRNA with electrostatic attraction under certain conditions, which can greatly improve the interception level of siRNA in NP and provide reliable support for its therapeutic effect. Therefore, it is widely concerned in the field of anti-tumor therapy and drug carrier research.[36] As illustrated in representative transmission electron microscopy (TEM) image (Figure 6B), PLGA-PEG (si-circROBO1) NPs were spherical. Subsequently, dynamic light scattering (DLS) was employed in the measurement of their size. The average diameter of PLGA-PEG (si-circROBO1) NPs was ~119.77 nm (Figure 6C) and the zeta potential was ~ −11.02 mV (Figure 6D). In addition, the stability of PLGA-PEG (si-circROBO1) NPs was evaluated by measuring particle size changes with DLS at various time points up to 96 h, and the results have shown that particle size does not change with times (Figure 6E). Next, we confirmed the knockdown efficiency in HCCLM9 cells. qRT-PCR results showed that more than 70% of circROBO1 expression could be suppressed by PLGA-PEG (si-circROBO1) NPs when siRNA dose was 36 nM (Figure 6F). Meanwhile, PLGA-PEG (si-circROBO1) NPs significantly suppressed the expression of circROBO1 at this dose compared to NPs and si-control NPs (Figure 6G). In addition, colony formation and EdU assays were conducted to evaluate the inhibiting proliferation ability of PLGA-PEG (si-circROBO1) NPs. The results consistently indicated that PLGA-PEG (si-circROBO1) NPs significantly decreased the proliferation of HCC cells (Figure 6H). Collectively, these results imply that circROBO1 can be regarded as a target for HCC treatment.

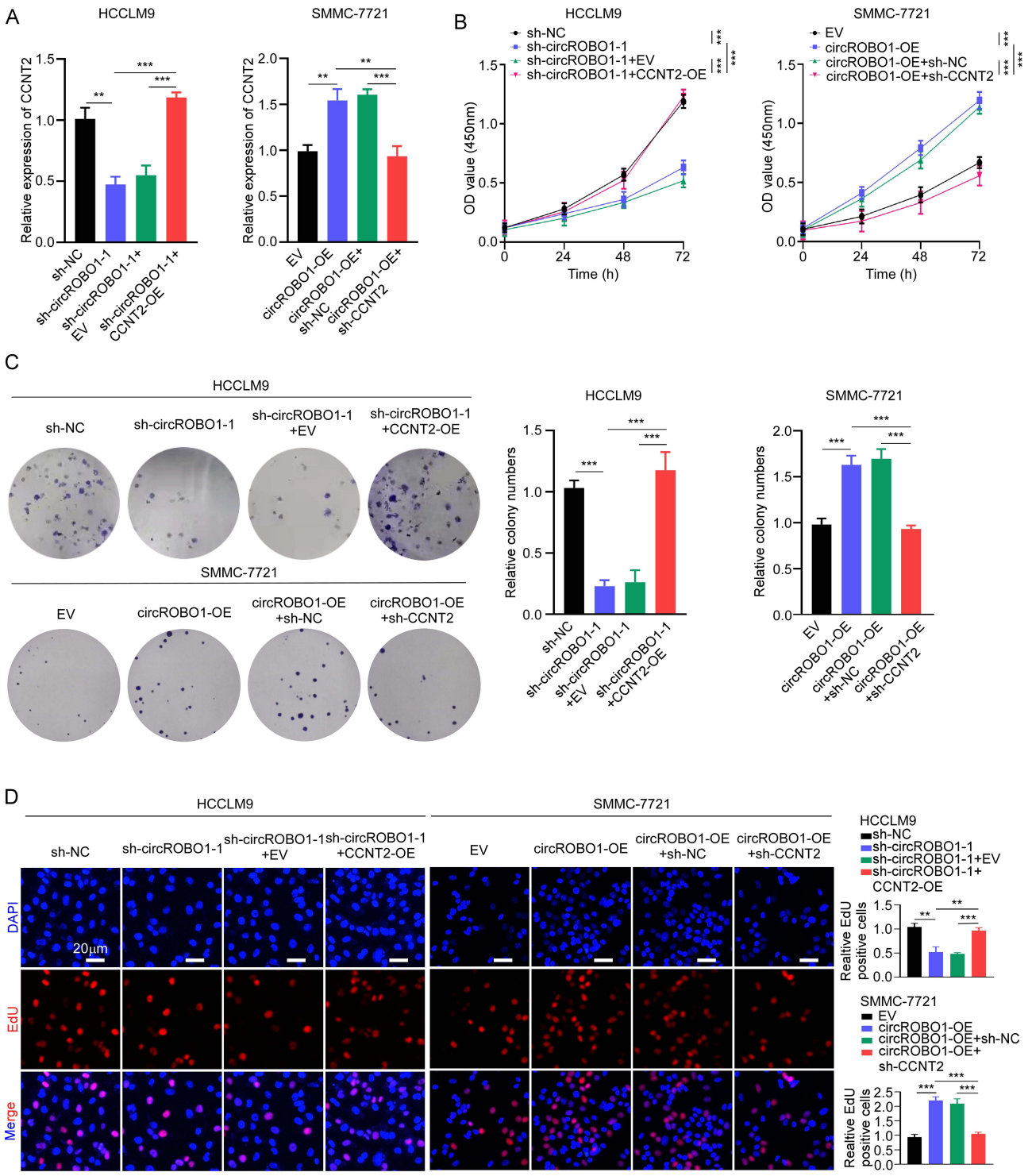

Figure 5 CircROBO1 promotes HCC proliferation by upregulating CCNT2 expression. (**A**) The relative expression of CCNT2 was detected in HCCLM9 and SMMC-7721 cells as indicated treatments. (**B**–**D**) The cell proliferative ability of HCCLM9 and SMMC-7721 cells as indicated treatments was detected by CCK8 (**B**), colony formation (**C**), and EdU (**D**) assays. Scale bar, 20 μm. Data were presented as means ±SD. ***P*<0.01; ****P*<0.001.

Anti-Tumor Efficacy and Toxicity Testing of PLGA-PEG (si-circROBO1) NPs in vivo

To test the potential of PLGA-PEG (si-circROBO1) NPs delivery in mice, pharmacokinetics (PK) and biodistribution (BioD) assays were performed. PK parameters were assessed by the injection of free Cy-5 si-circROBO1 or PLGA-PEG (Cy-5 si-circROBO1) NPs into nude mice based on tail vein and results implicated that PLGA-PEG (Cy-5 si-

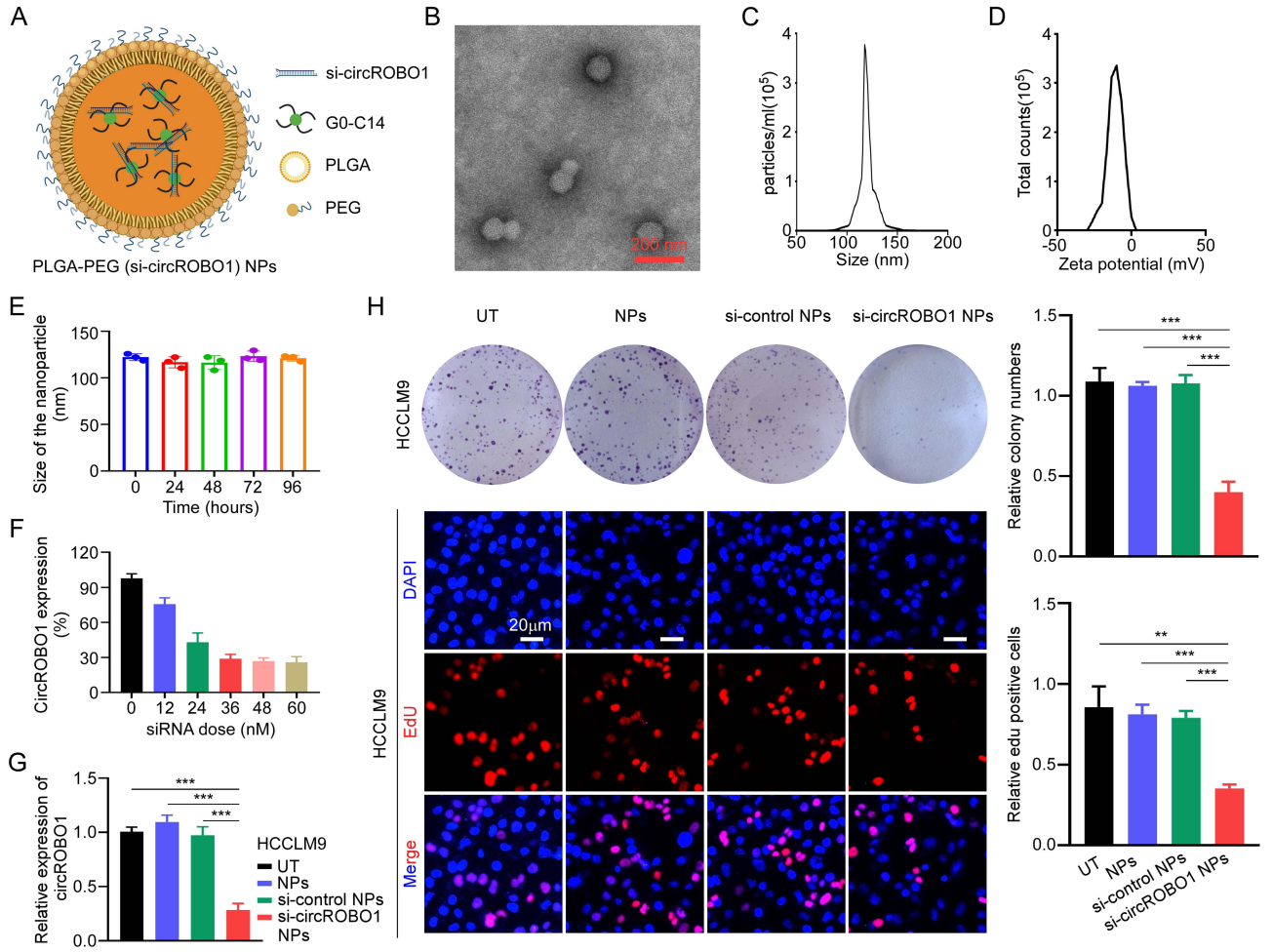

Figure 6 The biological characteristics of PLGA-PEG (si-circROBO1) NPs. (**A**) Schematic illustration of the PLGA-PEG (si-circROBO1) NPs. (**B**) Representative TEM image of PLGA-PEG (si-circROBO1) NPs. Scale bar, 200 nm. (**C**) Size distribution of the PLGA-PEG (si-circROBO1) NPs in the aqueous solution detected by Dynamic light scattering (DLS). (**D**) Zeta potential of PLGA-PEG (si-circROBO1) NPs in the aqueous solution . (**E**) In vitro stability of PLGA-PEG (si-circROBO1) NPs in 10% serum at 37°C was evaluated by measuring particle size changes with DLS at various time points up to 96 h. (**F**) The circROBO1 expression was determined by qRT-PCR in HCCLM9 cells which treated with PLGA-PEG (si-circROBO1) NPs at different siRNA doses. (**G**) The relative expression of circROBO1 was determined by qRT-PCR in HCCLM9 cells which treated with NPs, si-control NPs or si-circROBO1 NPs. (**H**) The proliferative ability of HCCLM9 cells which treated with NPs, si-control NPs or si-circROBO1 NPs was assessed by colony formation and EdU assays in vitro. Scale bar, 20 μm. Data were presented as means ±SD. $^{**}P<0.01$; $^{***}P<0.001$.

circROBO1) NPs had a more persistent blood circulation, while free si-circROBO1 was rapidly cleared (Figure 7A). We then tested the biodistribution of Cy-5 si-circROBO1 in HCC nude mice model after treating free Cy-5 si-circROBO1 and PLGA-PEG (Cy-5 si-circROBO1) NPs. The results of biodistribution indicated that PLGA-PEG (Cy-5 si-circROBO1) NPs had higher targeting effect on tumor sites (Figure 7B).

To test the anti-tumor efficacy of such kinds of NPs delivery in mice, HCCLM9 cells were injected into the abdominal wall of nude mice to construct xenograft tumor models, followed by tail vein injection of NPs, si-control NPs, or si-circROBO1 NPs with a dose of 700 μg/kg by intravenous (i.v.) injection every 3 days for 7 cycles. The results showed that tumor volume was significantly diminished in mice injected with si-circROBO1 NPs compared to NPs and si-control NPs injection (Figure 7C). Meanwhile, qRT-PCR results were in accordance with the knockdown of circROBO1 and CCNT2 expressions in xenografts treated with si-circROBO1 NPs (Figure 7D). During the whole treatment process, there were no significant changes in weights of the mice, which also reflected the high safety of this treatment and would not lead to systemic toxicity (Figure 7E).

Furthermore, systemic toxicity was assessed by H&E staining, and we found no distinct toxicity to liver, kidney, lung, spleen, and heart when injected intravenously with si-circROBO1 NPs (Figure 7F). Moreover, the index of ALT, AST, BUN, and Cr were conducted, excluding the presence of noticeable hepatotoxicity and renotoxicity (Figure 7G). Hence,

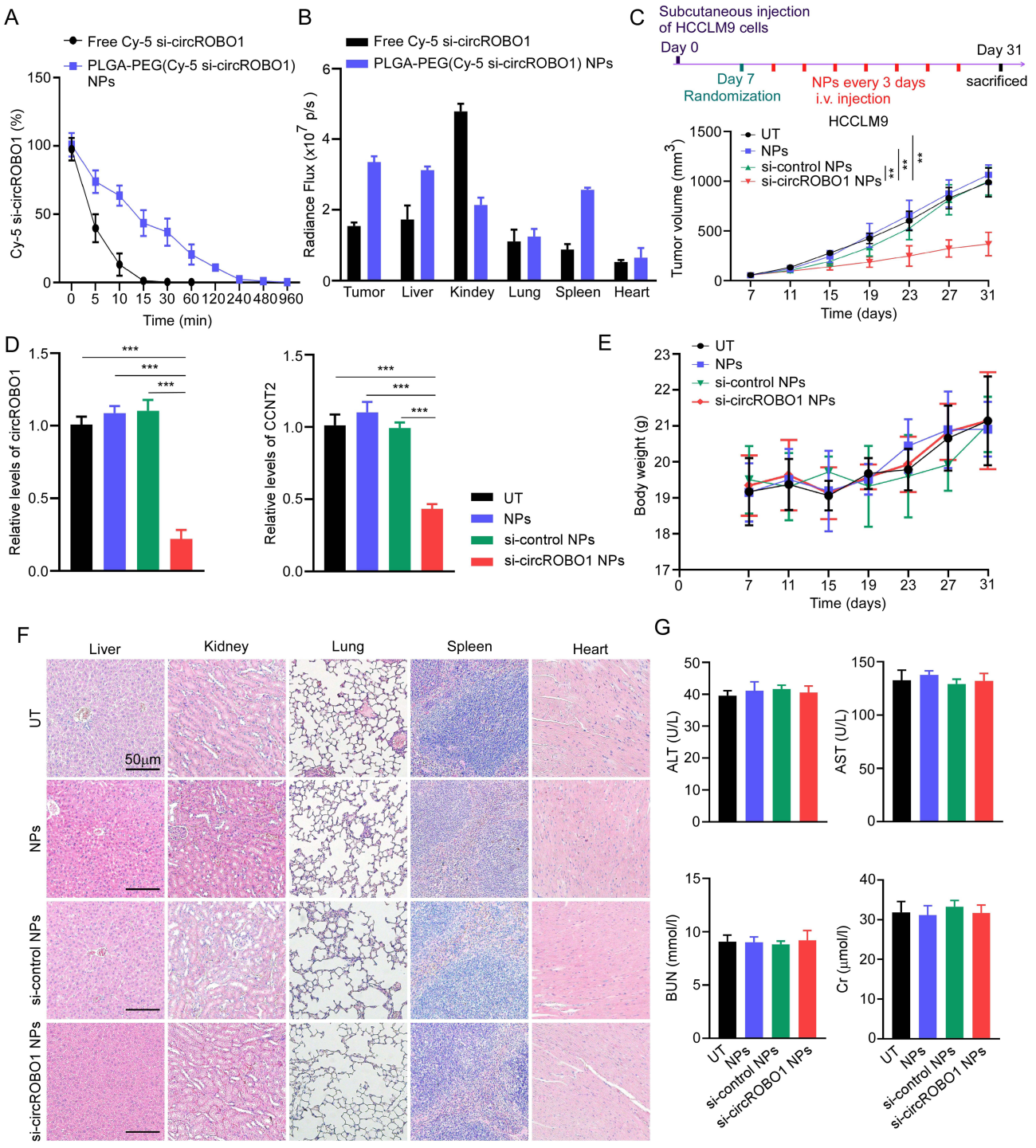

Figure 7 Anti-tumor efficacy and toxicity evaluation of PLGA-PEG (si-circROBO1) NPs in vivo. (**A**) Blood circulation profile of free Cy-5 si-circROBO1 and PLGA-PEG (Cy-5 si-circROBO1) NPs. (**B**) Biodistribution of free Cy-5 si-circROBO1 and PLGA-PEG (Cy-5 si-circROBO1) NPs injections on major organs and tumors after 24 h of treatment. (**C**) Timeline of tumor implantation and treatment schedule in the HCC xenograft tumor-bearing nude mice. Tumor growth profile of the HCC xenograft tumor-bearing mice treated with NPs, si-control NPs and si-circROBO1 NPs. (**D**) The relative expression of circROBO1 and CCNT2 was evaluated by qRT-PCR in subcutaneous xenograft tumor tissues as indicated treatments. (**E**) Changes of mouse body weight during experimental period in subcutaneous xenograft tumor models. (**F**) Representative H&E staining of major organs including the liver, kidney, lung, spleen, and heart in subcutaneous xenograft tumor models, scale bar, 50 μm. (**G**) Blood ALT, AST, BUN, and Cr levels in subcutaneous xenograft tumor models. Data were presented as means ±SD. ***P*<0.01; ****P*<0.001.

https://doi.org/10.2147/IJN.S399318 DovePress

the above results demonstrate that PLGA-PEG (si-circROBO1) NPs significantly suppressed the proliferation of HCC cells in vivo, while they did not exhibit apparent toxicity to major organs in vivo.

Discussion

Accumulating studies indicate that circRNAs are differentially expressed in HCC, and these differentially expressed circRNAs may play the role of biomarkers in cancer diagnosis and prognosis.[37,38] However, the molecular mechanisms for circRNAs in HCC are still largely elusive. Hence, we investigated the function and underlying mechanism of the upregulated circROBO1 expression in HCC by screening the differentially expressed circRNAs (DECs) between HCC tissues and paired nontumor liver tissues.

Herein, there appeared to be a noticeable upregulation in circROBO1 level in HCC tissues, and higher expression of circROBO1 implied a poor prognosis. Besides, circROBO1 exhibited stable performance compared to linear ROBO1 and was preferentially localized in the cytoplasm. To the best of our knowledge, targeting circROBO1 was first found to have anti-HCC activity, which extended previous studies of other circRNAs. Further research revealed that circROBO1 overexpression promoted HCC cell proliferation and increased the number of G2/M phase tumor cells.

Most circRNAs were reported to function as a ceRNA to sponge several miRNAs and then suppressed these miRNAs activity, which enhanced the expression of miRNA-targeted genes.[39–41] Such as, circTOLLIP can sponge miR-516a-5p to upregulate PBX3 expression and promote epithelial-to-mesenchymal transition in HCC.[42] In our study, we further confirmed that miR-130a-5p was capable of binding to circROBO1 by luciferase activity and AGO2-RIP assays. Furthermore, the circROBO1 sponged endogenous miR-130a-5p to inhibit miR-130a-5p activity, and miR-130a-5p inhibitor could reverse the inhibitory effect of circROBO1 silence on cell proliferation in HCC cells. Collectively, our data indicated that circROBO1 could serve as a miRNA sponge for miR-130a-5p, and our findings may provide a novel insight into the role of circROBO1 on the circRNA/miRNA regulatory network to mediate the progression of HCC.

miRNAs usually regulate target genes expression by interacting with the 3'-UTR,[43–46] therefore we investigated the seven potential target genes of miR-130a-5p in HCC. Among them, CCNT2 was associated with cell proliferation and was closely related to many cancers progression, such as acute myeloid leukemia and gastric cancer.[19,33] CCNT2 is a kind of conserved cyclin family that has feature of a dramatic periodicity in protein abundance through the cell cycle. In this study, we found that circROBO1 abolished the suppression of CCNT2 mediated by miR-130a-5p, and the knockdown of CCNT2 also eliminated the promotion of proliferation induced by circROBO1 overexpression. Hence, the above findings firstly suggested that circROBO1/miR-130a-5p/CCNT2 axis might be an important regulator in the development of HCC.

The practicality and prospect of NP-targeted siRNA delivery for cancer nanotherapy have been accepted.[22] Liposomes and viral vectors that activate toxicity but fail to maintain sustained release of siRNAs are not well considered as potential carriers for siRNA delivery. With the approval of the FDA, PLGA has attracted extensive attention in the development of drugs related to nanoplatform carriers, and PLGA is applied to siRNA delivery due to its advantages such as good safety and biodegradability. For example, PLGA can deliver EPAS1 siRNA to treat pancreatic cancer.[47] In this study, we developed a kind of PLGA nano-carrier loaded with circROBO1 siRNA for HCC treatment. Additionally, since miRNAs have multiple mRNA targets, specificity of nanoparticle encapsulating siRNA is more accurate than miRNA.[48] Moreover, our results showed that PLGA-PEG (si-circROBO1) NPs could protect si-circROBO1 from early degradation, so it was beneficial to improve the uptake efficacy. Importantly, animal study suggested that the uptake of NPs into tumor cells was enhanced, which can accelerate the increasing number of NPs in the tumor. Also, functional assays indicated that PLGA-PEG (si-circROBO1) NPs group inhibited HCC cell proliferation compared with the control group. Additionally, the results of H&E staining and blood biochemical verified absence of distinct toxic side effects. Given that cancer cells have a high concentration of endogenous reactive oxidative stress (ROS), therefore the combination of siRNA-nanoparticles and antioxidant nanoparticle platforms or carbon nanotubes can potentially improve the efficacy and safety for HCC treatment and diagnosis for future research.[49–51]

Conclusion

In our study, we performed a comprehensive investigation of the roles, molecular mechanisms, and target therapy of circROBO1 in HCC. The findings showed that circROBO1 overexpression was associated with worse OS and RFS in

patients with HCC. Mechanistically, we firstly found that circROBO1 overexpression facilitated HCC cell proliferation through the sponge miR-130a-5p, leading to increased CCNT2 expression. More importantly, we constructed an effective nanoplatform encapsulating circROBO1 siRNA for HCC therapy and PLGA-PEG (si-circROBO1) NPs exhibited anti-HCC activity in vitro and in vivo (Supplementary Figure 3). Taken together, targeting circROBO1 might represent a novel therapeutic strategy for the treatment of HCC.

Ethics Approval and Consent to Participate

This project was approved to participate by the Ethics Committee of the First Affiliated Hospital of Gannan Medical University.

Data Sharing Statement

The data presented in this study are available on request from the corresponding author.

Funding

This study was supported by grants from the China Postdoctoral Science Foundation Funded Project (2021M703685) and Shenzhen Science and Technology Innovation Commission based research (JCYJ20220530144404010, JCYJ20220530144404011).

Disclosure

The authors declare no conflict of interest.

References

1. Sung H, Ferlay J, Siegel RL, et al. Global cancer statistics 2020: GLOBOCAN estimates of incidence and mortality worldwide for 36 cancers in 185 countries. *Ca Cancer J Clin*. 2021;71(3):209–249. doi:10.3322/caac.21660
2. Xu M, Yang L, Lin Y, et al. Emerging nanobiotechnology for precise theranostics of hepatocellular carcinoma. *J Nanobiotechnol*. 2022;20(1):427. doi:10.1186/s12951-022-01615-2
3. Ding J, Wen Z. Survival improvement and prognosis for hepatocellular carcinoma: analysis of the SEER database. *BMC Cancer*. 2021;21(1):1157. doi:10.1186/s12885-021-08904-3
4. Chen L, Shan G. CircRNA in cancer: fundamental mechanism and clinical potential. *Cancer Lett*. 2021;505:49–57. doi:10.1016/j.canlet.2021.02.004
5. Zhang Q, Wang W, Zhou Q, et al. Roles of circRNAs in the tumour microenvironment. *Mol Cancer*. 2020;19(1):14. doi:10.1186/s12943-019-1125-9
6. Chen M, Liu Q, Song M, et al. CircCLTH promotes skeletal muscle development and regeneration. *Epigenetics*. 2022;17(13):2296–2317. doi:10.1080/15592294.2022.2117115
7. Wang J, Wen Y, Xu J, et al. CircRIMKLB promotes myoblast proliferation and inhibits differentiation by sponging miR-29c to release KCNJ12. *Epigenetics*. 2022;17(12):1686–1700. doi:10.1080/15592294.2022.2058211
8. Shen X, Tang J, Huang Y, et al. CircRNF111 contributes to adipocyte differentiation by elevating PPARγ expression via miR-27a-3p. *Epigenetics*. 2022:1–15. doi:10.1080/15592294.2022.2145058
9. Li J, Xu Q, Huang ZJ, et al. CircRNAs: a new target for the diagnosis and treatment of digestive system neoplasms. *Cell Death Dis*. 2021;12(2):205. doi:10.1038/s41419-021-03495-0
10. Mo Z, Li R, Cao C, et al. Splicing factor SNRPA associated with microvascular invasion promotes hepatocellular carcinoma metastasis through activating NOTCH1/Snail pathway and is mediated by circSEC62/miR-625-5p axis. *Environ Toxicol*. 2023. doi:10.1002/tox.23745
11. Feng Y, Feng L, Yu D, et al. srGAP1 mediates the migration inhibition effect of Slit2-Robo1 in colorectal cancer. *J Exp Clin Cancer Res*. 2016;35(1):191. doi:10.1186/s13046-016-0469-x
12. Chang PH, Hwang-Verslues WW, Chang YC, et al. Activation of Robo1 signaling of breast cancer cells by Slit2 from stromal fibroblast restrains tumorigenesis via blocking PI3K/AKt/β-catenin pathway. *Cancer Res*. 2012;72(18):4652–4661. doi:10.1158/0008-5472.CAN-12-0877
13. Ito H, Funahashi S, Yamauchi N, et al. Identification of ROBO1 as a novel hepatocellular carcinoma antigen and a potential therapeutic and diagnostic target. *Clin Cancer Res*. 2006;12(11 Pt 1):3257–3264. doi:10.1158/1078-0432.CCR-05-2787
14. Wang Z, Yang L, Wu P, et al. The circROBO1/KLF5/FUS feedback loop regulates the liver metastasis of breast cancer by inhibiting the selective autophagy of afadin. *Mol Cancer*. 2022;21(1):29. doi:10.1186/s12943-022-01498-9
15. Zhang Y, Wang Y, Ji H, et al. The interplay between noncoding RNA and YAP/TAZ signaling in cancers: molecular functions and mechanisms. *J Exp Clin Cancer Res*. 2022;41(1):202. doi:10.1186/s13046-022-02403-4
16. Liu Y, Liu X, Lin C, et al. Noncoding RNAs regulate alternative splicing in cancer. *J Exp Clin Cancer Res*. 2021;40(1):11. doi:10.1186/s13046-020-01798-2
17. Li C, Zhao W, Pan X, et al. LncRNA KTN1-AS1 promotes the progression of non-small cell lung cancer via sponging of miR-130a-5p and activation of PDPK1. *Oncogene*. 2020;39(39):6157–6171. doi:10.1038/s41388-020-01427-4
18. Kohoutek J, Li Q, Blazek D, et al. Cyclin T2 is essential for mouse embryogenesis. *Mol Cell Biol*. 2009;29(12):3280–3285. doi:10.1128/MCB.00172-09

19. Ke S, Li RC, Lu J, et al. MicroRNA-192 regulates cell proliferation and cell cycle transition in acute myeloid leukemia via interaction with CCNT2. *Int J Hematol*. 2017;106(2):258–265. doi:10.1007/s12185-017-2232-2
20. Xin Y, Huang M, Guo WW, et al. Nano-based delivery of RNAi in cancer therapy. *Mol Cancer*. 2017;16(1):134. doi:10.1186/s12943-017-0683-y
21. Ye Z, Zhu Z, Xie J, et al. Hsa_circ_0000069 knockdown inhibits tumorigenesis and exosomes with downregulated hsa_circ_0000069 suppress malignant transformation via inhibition of STIL in pancreatic cancer. *Int J Nanomed*. 2020;15:9859–9873. doi:10.2147/IJN.S279258
22. El-Say KM, El-Sawy HS. Polymeric nanoparticles: promising platform for drug delivery. *Int J Pharm*. 2017;528(1–2):675–691. doi:10.1016/j.ijpharm.2017.06.052
23. Sousa AR, Oliveira AV, Oliveira MJ, et al. Nanotechnology-based siRNA delivery strategies for metastatic colorectal cancer therapy. *Int J Pharm*. 2019;568:118530. doi:10.1016/j.ijpharm.2019.118530
24. Kaul G, Amiji M. Long-circulating poly (ethylene glycol)-modified gelatin nanoparticles for intracellular delivery. *Pharm Res*. 2002;19(7):1061–1067. doi:10.1023/a:
25. Rahman M, Almalki WH, Afzal O, et al. Cationic solid lipid nanoparticles of resveratrol for hepatocellular carcinoma treatment: systematic optimization, in vitro characterization and preclinical investigation. *Int J Nanomedicine*. 2020;15:9283–9299. doi:10.2147/IJN.S277545
26. Mao Y, Yan R, Li A, et al. Lentiviral vectors mediate long-term and high efficiency transgene expression in HEK 293T cells. *Int J Med Sci*. 2015;12(5):407–415. doi:10.7150/ijms.11270
27. Cohen-Sela E, Chorny M, Koroukhov N, et al. A new double emulsion solvent diffusion technique for encapsulating hydrophilic molecules in PLGA nanoparticles. *J Control Release*. 2009;133(2):90–95. doi:10.1016/j.jconrel.2008.09.073
28. Saw PE, Zhang A, Nie Y, et al. Tumor-associated fibronectin targeted liposomal nanoplatform for cyclophilin a siRNA delivery and targeted malignant glioblastoma therapy. *Front Pharmacol*. 2018;9:1194. doi:10.3389/fphar.2018.01194
29. Liu H, Yuan M, Liu Y, et al. Self-monitoring and self-delivery of self-assembled fluorescent nanoparticles in cancer therapy. *Int J Nanomedicine*. 2021;16:2487–2499. doi:10.2147/IJN.S294279
30. Wei W, Zhang X, Chen X, et al. Smart surface coating of drug nanoparticles with cross-linkable polyethylene glycol for bio-responsive and highly efficient drug delivery. *Nanoscale*. 2016;8(15):8118–8125. doi:10.1039/c5nr09167e
31. Zhao X, Cai Y, Xu J. Circular RNAs: biogenesis, mechanism, and function in human cancers. *Int J Mol Sci*. 2019;20:16. doi:10.3390/ijms20163926
32. Liu B, Li J, Cairns MJ. Identifying miRNAs, targets and functions. *Brief Bioinform*. 2014;15(1):1–19. doi:10.1093/bib/bbs075
33. Chen X, Zhang L, Song Q, et al. MicroRNA-216b regulates cell proliferation, invasion and cycle progression via interaction with cyclin T2 in gastric cancer. *Anticancer Drugs*. 2020;31(6):623–631. doi:10.1097/CAD.0000000000000915
34. Li L, He K, Chen S, et al. Circ_0001175 promotes hepatocellular carcinoma cell proliferation and metastasis by regulating miR-130a-5p. *Onco Targets Ther*. 2020;13:13315–13327. doi:10.2147/OTT.S262408
35. Motlaq VF, Knudsen KD, Nyström B. Effect of PEGylation on the stability of thermoresponsive nanogels. *J Colloid Interface Sci*. 2018;524:245–255. doi:10.1016/j.jcis.2018.04.024
36. Bai X, Zhao G, Chen Q, et al. Inhaled siRNA nanoparticles targeting IL11 inhibit lung fibrosis and improve pulmonary function post-bleomycin challenge. *Sci Adv*. 2022;8(25):eabn7162. doi:10.1126/sciadv.abn7162
37. Hao X, Zhang Y, Shi X, et al. CircPAK1 promotes the progression of hepatocellular carcinoma via modulation of YAP nucleus localization by interacting with 14-3-3ζ. *J Exp Clin Cancer Res*. 2022;41(1):281. doi:10.1186/s13046-022-02494-z
38. Li Y, Wu A, Chen L, et al. Hsa_circ_0000098 is a novel therapeutic target that promotes hepatocellular carcinoma development and resistance to doxorubicin. *J Exp Clin Cancer Res*. 2022;41(1):267. doi:10.1186/s13046-022-02482-3
39. Xu YP, Dong ZN, Wang SW, et al. CircHMGCS1-016 reshapes immune environment by sponging miR-1236-3p to regulate CD73 and GAL-8 expression in intrahepatic cholangiocarcinoma. *J Exp Clin Cancer Res*. 2021;40(1):290. doi:10.1186/s13046-021-02095-2
40. Song LN, Qiao GL, Yu J, et al. Hsa_circ_0003998 promotes epithelial to mesenchymal transition of hepatocellular carcinoma by sponging miR-143-3p and PCBD1. *J Exp Clin Cancer Res*. 2020;39(1):114. doi:10.1186/s13046-020-01576-0
41. Zhao Z, Song J, Tang B, et al. CircSOD2 induced epigenetic alteration drives hepatocellular carcinoma progression through activating JAK2/STAT3 signaling pathway. *J Exp Clin Cancer Res*. 2020;39(1):259. doi:10.1186/s13046-020-01769-7
42. Liu Y, Song J, Zhang H, et al. EIF4A3-induced circTOLLIP promotes the progression of hepatocellular carcinoma via the miR-516a-5p/PBX3/EMT pathway. *J Exp Clin Cancer Res*. 2022;41(1):164. doi:10.1186/s13046-022-02378-2
43. Lv Q, Wang G, Zhang Y, et al. CircAGAP1 promotes tumor progression by sponging miR-15-5p in clear cell renal cell carcinoma. *J Exp Clin Cancer Res*. 2021;40(1):76. doi:10.1186/s13046-021-01864-3
44. Liao Z, Zhang H, Su C, et al. Long noncoding RNA SNHG14 promotes hepatocellular carcinoma progression by regulating miR-876-5p/SSR2 axis. *J Exp Clin Cancer Res*. 2021;40(1):36. doi:10.1186/s13046-021-01838-5
45. Huang Q, Zhang F, Fu H, et al. Epigenetic regulation of miR-518a-5p-CCR6 feedback loop promotes both proliferation and invasion in diffuse large B cell lymphoma. *Epigenetics*. 2021;16(1):28–44. doi:10.1080/15592294.2020.1786317
46. Nair PS, Raijas P, Ahvenainen M, et al. Music-listening regulates human microRNA expression. *Epigenetics*. 2021;16(5):554–566. doi:10.1080/15592294.2020.1809853
47. Pan X, Zhu Q, Sun Y, et al. PLGA/poloxamer nanoparticles loaded with EPAS1 siRNA for the treatment of pancreatic cancer in vitro and in vivo. *Int J Mol Med*. 2015;35(4):995–1002. doi:10.3892/ijmm.2015.2096
48. Lam JK, Chow MY, Zhang Y, et al. siRNA versus miRNA as therapeutics for gene silencing. *Mol Ther Nucleic Acids*. 2015;4(9):e252. doi:10.1038/mtna.2015.23
49. Ahmadian E, Janas D, Eftekhari A, et al. Application of carbon nanotubes in sensing/monitoring of pancreas and liver cancer. *Chemosphere*. 2022;302:134826. doi:10.1016/j.chemosphere.2022.134826
50. Ahmadian E, Khosroushahi AY, Eftekhari A, et al. Novel angiotensin receptor blocker, azilsartan induces oxidative stress and NFKB-mediated apoptosis in hepatocellular carcinoma cell line HepG2. *Biomed Pharmacother*. 2018;99:939–946. doi:10.1016/j.biopha.2018.01.117
51. Ahmadian E, Babaei H, Mohajjel NA, et al. Venlafaxine-induced cytotoxicity towards isolated rat hepatocytes involves oxidative stress and mitochondrial/lysosomal dysfunction. *Adv Pharm Bull*. 2016;6(4):521–530. doi:10.15171/apb.2016.066